Meccanica (2013) 48:1053–1070
DOI 10.1007/s11012-012-9651-1

Buckling and vibration of axially functionally graded nonuniform beams using differential transformation based dynamic stiffness approach

S. Rajasekaran

Received: 7 June 2012 / Accepted: 22 October 2012 / Published online: 2 November 2012

Abstract The free vibration of axially functionally graded (FG) non-uniform beams with different boundary conditions is studied using Differential Transformation (DT) based Dynamic Stiffness approach. This method is capable of modeling any beam (Timoshenko or Euler, centrifugally stiffened or not) whose cross sectional area, moment of Inertia and material properties vary along the beam. The effectiveness of the method is confirmed by comparing the present results with existing closed form solutions and numerical results. In FG beams, flexural rigidity and mass density may take majority of functions including polynomials, trigonometric and exponential functions (converted to polynomial expressions). DT based Dynamic stiffness approach is proved to be a versatile and simple approach compared to many other methods already proposed.

Keywords Timoshenko beam · Euler beam · Bending stiffness · Mass density · Functionally graded material · Nonuniform beam

Nomenclature

A_0	Area of the section at the root
$A(x)$	Cross sectional area at any section
$b(x)$	Breadth of the cross section at any section
$d(x) = E(x)I(x)$	Flexural rigidity at any section
$E(x)$	Modulus of elasticity of the axially graded material at any section
e	Taper ratio
$G(x)$	Modulus of rigidity at any section
$h(x)$	Depth of the cross section at any section
$I(x)$	Moment of Inertia at any section
I_0	Moment of Inertia of the section at the root
$K(x) = \kappa A(x)G(x)$	Shear rigidity at any section
$\mathbf{K}$	Structural stiffness matrix
$\mathbf{KG}$	Geometric stiffness matrix
L	Length of the beam
$mr = 1$	Depth taper only
$mr = 2$	Both width and depth taper
M_T	Tip mass at the free end
$M(x)$	Moment at any section
$\mathbf{M}$	Mass matrix
nt	Number of terms
nr	Material non-homogeneity factor
$P(x)$	Centrifugal force or compressive load
$p(x)$	Lateral load
$p = \frac{PL^2}{EI_0}$	Buckling load parameter
R	Hub radius
s	Summation index
T	Typical material property
T_a, T_z	Typical material property for Alumina and Zirconia respectively
$V(x)$	Shear force
w	Lateral deflection of the centre line of the beam

S. Rajasekaran (✉)
PSG College of Technology, Coimbatore, India
e-mail: srs.civ@gapps.psgtech.ac.in

x, y and z	Cartesian coordinate axes
$y(x)$	Function
β	Tip mass parameter
$\delta = R/L$	Non-dimensional parameter for hub radius
	$\eta = \sqrt{\Omega^2 + \omega^2}$
κ	Shear correction factor
λ	Rotating speed parameter where
	$\lambda = \Omega\sqrt{\frac{\rho_0 A_0 L^4}{E_0 I_0}}$
μ	Natural frequency parameter where
	$\mu = \omega\sqrt{\frac{\rho_0 A_0 L^4}{E_0 I_0}}$
Ω	Angular rotation speed in radians/sec
φ	Shape function for θ
$\rho(x)$	Mass density of axially graded material at any section
$\boldsymbol{\psi}$	Shape function for bending rotation
θ	Bending rotation
ω	Natural frequency
$\xi = \frac{x}{L}$	Non-dimensional variable
ς	Damping factor
$\nabla = \frac{\mathrm{d}}{\mathrm{d}x}$	Operator

1 Introduction

There has been a great interest in the analysis of the free vibration characteristics of elastic structures such as turbine, compressor or helicopter blades, spinning spacecraft and satellite booms rotating with constant angular velocity. For a relatively long blade the simplest response is the Euler Bernoulli beam model (EBM). In some cases, these shafts are stubby and when the higher modes in bending vibrations are considered, Timoshenko beam theory (TBT) is employed. The only distinction between the above two theories being shear deformation and rotary inertia are considered in TBT in addition to centrifugal force. With the above, functionally graded material (FGM) complicates the issue.

FGM are multiphase composites with volume fraction of phase varying through a direction. FGM was first proposed by material scientists in Sendai area in Japan in 1984 [1, 2] as thermal barrier material. Since then, these materials have been employed in many engineering application fields such as aircrafts, space vehicles, defense industries, electronic and biomedical sectors. For functionally graded beams, gradient variation may be oriented in cross section, or in the axial direction. But in this research, gradient variation is considered in axial direction.

Semi-inverse method was used to study beam with axially FGM by Elishakoff and his co-workers [3, 4]. Many researchers have used numerical techniques such as Frobenius and Rayleigh-Ritz methods [5–8]. Spectral finite element method (SFEM) also called dynamic stiffness method has been applied by Vinod et al. [9], Doyle [10] to provide a high accuracy using less number of elements. Wright et al. [11] applied the Frobenius method (extended power series method) and solved for natural frequencies of both uniform and tapered rotating beam with cantilever or hinged boundary conditions, in which tapered beam has a linear variation of mass and flexural stiffness along the span of the beam. Huang and Li [12] studied the free vibration of nonuniform axially FG beams by transforming governing equation to Fredholm integral equation.

For Timoshenko beams, Mabie and Rogers [13] solved the differential equation of vibration of a tapered beam by using Bessel functions. Downs [14] employed a dynamic discretization technique to calculate the natural frequency of a tapered Timoshenko beam. Finite element technique was used by Gupta and Rao [15], Dawe [16], To [17], and Lees and Thomas [18] to study the effect of shear deformation and rotary inertia on the modal frequency of a tapered beam. The free vibration characteristics of rotating Timoshenko beams have also been extensively studied by Lee and Lin [19], Du et al. [20], Nagaraj [21] and Lin and Hsiao [22].

The vibration of tapered beams has also been studied by other methods such as the modified differential quadrature method by Choi and Chou 2001 [23], the spline interpolation technique by Irie et al. [24], the transfer matrix approach by Irie et al. [25] and the method of Frobenius by Lee and Lin [26]. Shahba et al. [27] applied FEM using Hermitian polynomials to study the free vibration and stability of tapered axially functionally graded beam. Attarnejad et al. [28] used basic displacement functions (BDF) for free vibration analysis of non-prismatic Timoshenko beams. Attarnejad and Shahba [29, 30] used basic displacement functions to study the free vibration of centrifugally stiffened tapered beams.

In the present paper, we adopt the Differential transformation (DT) based dynamic stiffness method to study the buckling and vibration characteristics of axially FG tapered Euler and Timoshenko beams (centrifugally stiffened or not) by considering four first order differential equations. Zhou [31] was the first

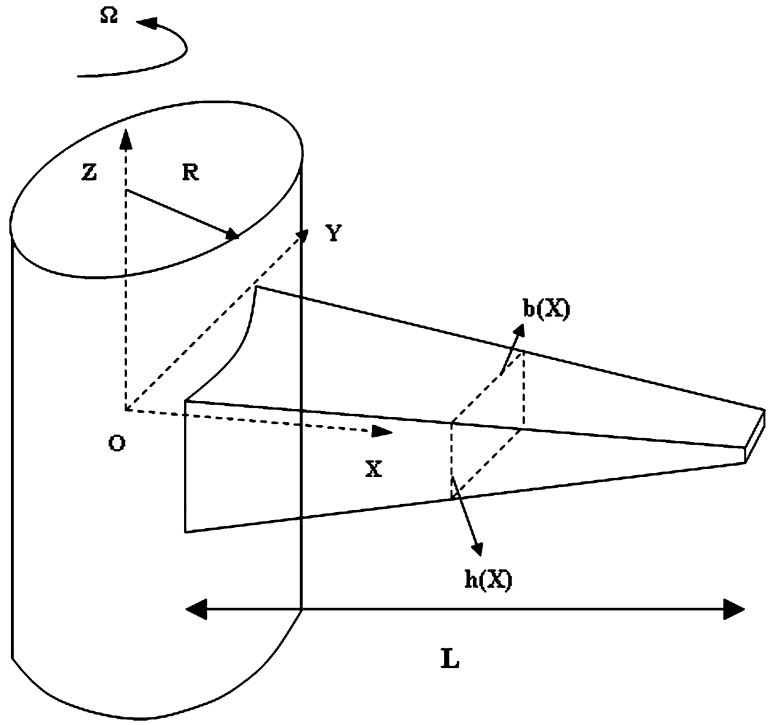

Fig. 1 Configuration of functionally graded tapered rotating cantilever beam

one to use differential transformation method (DTM) in engineering applications. Since DTM is an efficient tool for solving nonlinear or parameter varying systems, it has gained much attention by several researchers such as Chen and Ju [32], Arikoglu and Ozhol [33] and Bert and Zeng [34].

However, DT method considered in this paper is much different from other investigators.

(a) DT based dynamic stiffness method does not pose any restriction on both the type of material gradation and variation of the cross section profile and hence they could cover most of the engineering problems dealing with axially FG beams.
(b) The technique is directly used to get the shape functions for displacements and bending rotations and hence stiffness, geometric stiffness and mass matrices can be arrived at. Using finite element procedure, these matrices are assembled to form global matrices and applying boundary conditions one can solve for the free and forced vibration and stability problems for the beams and predict the natural frequency and buckling load more precisely in comparison with previous works.
(c) DT replaces power series in establishing the dynamic stiffness of beams.

2 Governing differential equations

In Fig. 1, a cantilever beam of length L, which is rigidly fixed on the periphery of a rigid hub of radius R is shown. The hub is assumed to rotate about its vertical axis 'z' at a constant angular speed Ω. We consider the right hand Cartesian system and the origin is located at the left end of the beam (centre of the hub). The following assumptions are made [35].

(1) The x axis coincides with the neutral axis of the beam in the un-deformed position.
(2) The beam cross section is doubly symmetric.
(3) The out-of-plane displacements are small and neglected.
(4) The cross sections which are initially perpendicular to the neural axis will remain plane but not perpendicular after deformation for Timoshenko beams.
(5) Coriolis effects are very small and neglected in case of centrifugally stiffened beam.

Based on Timoshenko beam theory, governing differential equation for free transverse vibration of axially FG tapered rotating beams were derived by Kaya [35] as well as Banerjee [36]. Here we will not repeat the derivation and we give only governing equations and the interested reader may consult Refs. [35, 36].

The shear force $\underline{V} = \underline{V}(x,t)$ at any section including shear deformation is given by

$$\underline{V}(x,t) = P(x)\frac{\mathrm{d}\underline{w}}{\mathrm{d}x} + K(x)\left(\frac{\mathrm{d}\underline{w}}{\mathrm{d}x} - \underline{\theta}\right) \tag{1}$$

where centrifugal force $P(x)$ varies along the span wise direction of the beam and is given by

$$P(x) = \int_x^L \rho(x)A(x)\Omega^2(R+x)\,\mathrm{d}x + M_T\Omega^2 L(1+\delta) \tag{2}$$

where $K(x)$ = shear rigidity given by $K(x) = \kappa \times A(x)G(x)$ only for Timoshenko beams and κ = shear correction factor depending on the cross section (values of κ for circular and rectangular cross section are 2/3 and 5/6). All the notations are defined in Nomenclature.

In case of buckling problems

$$\underline{V}(x,t) = -P(x)\frac{\mathrm{d}\underline{w}}{\mathrm{d}x} + K(x)\left(\frac{\mathrm{d}\underline{w}}{\mathrm{d}x} - \underline{\theta}\right) \tag{3}$$

where $P(x)$ is the compressive load at any section.

The bending moment $\underline{M} = \underline{M}(x,t)$ at any section is given by

$$\underline{M}(x,t) = d(x)\frac{\mathrm{d}\underline{\theta}}{\mathrm{d}x} \tag{4}$$

where $d(x) = E(x)I(x)$, the bending stiffness.

The equations of motion are obtained as

$$\frac{\mathrm{d}\underline{M}(x,t)}{\mathrm{d}x} + \rho(x)I(x)\Omega^2\underline{\theta} + K(x)\left(\frac{\mathrm{d}\underline{w}}{\mathrm{d}x} - \underline{\theta}\right) - \rho(x)I(x)\ddot{\underline{\theta}} = 0 \tag{5}$$

and

$$\frac{\mathrm{d}\underline{V}(x,t)}{\mathrm{d}x} - \rho(x)A(x)\ddot{\underline{w}} = p(x,t) \tag{6}$$

where

$$\ddot{\underline{\theta}} = \frac{\mathrm{d}^2\underline{\theta}}{\mathrm{d}t^2} \quad \text{and} \quad \ddot{\underline{w}} = \frac{\mathrm{d}^2\underline{w}}{\mathrm{d}t^2} \tag{7}$$

Sinusoidal variation for transverse displacement and bending rotation with circular frequency ω (assuming the lateral load, $p(x,t) = 0$) is given by

$$\underline{w}(x,t) = w\sin(\omega t + \phi); \quad \underline{\theta}(x,t) = \theta\sin(\omega t + \phi) \tag{8a}$$

$$\underline{M}(x,t) = M\sin(\omega t + \phi); \quad \underline{V}(x,t) = V\sin(\omega t + \phi) \tag{8b}$$

where w, θ, M and V are functions of x only and the variables with under score are functions of x and t.

Substituting Eqs. (8a), (8b) in Eqs. (4) and (5) we get

$$\frac{\mathrm{d}M(x)}{\mathrm{d}x} + \rho(x)I(x)\Omega^2\theta + K(x)\left(\frac{\mathrm{d}w}{\mathrm{d}x} - \theta\right) = -\omega^2\rho(x)I(x)\theta = 0 \tag{9a}$$

$$\frac{\mathrm{d}V(x)}{\mathrm{d}x} = -\omega^2\rho(x)A(x)w \tag{9b}$$

Equations (1), (3), (9a) and (9b) are written in matrix form as

$$\begin{bmatrix} \nabla & 0 & 0 & 0 \\ 0 & \nabla & -K(x)+\rho(x)I(x)\Omega^2 & K(x)\nabla \\ 0 & -\frac{1}{d(x)} & \nabla & 0 \\ -1 & 0 & -K(x) & (P(x)+K(x))\nabla \end{bmatrix} \times \begin{Bmatrix} V \\ M \\ \theta \\ w \end{Bmatrix} = -\omega^2 \begin{bmatrix} 0 & 0 & 0 & \rho(x)A(x) \\ 0 & 0 & \rho(x)I(x) & 0 \\ 0 & 0 & 0 & 0 \\ 0 & 0 & 0 & 0 \end{bmatrix} \begin{Bmatrix} V \\ M \\ \theta \\ w \end{Bmatrix} \tag{10}$$

In Eq. (10), for buckling problems $P(x)$ is to be substituted as $-P(x)$ where $\nabla = \frac{\mathrm{d}}{\mathrm{d}x}$ with boundary conditions ($V = 0$ or $w = 0$; $M = 0$ or $\theta = 0$ at $x = 0$ and $x = L$). It is to be noted that for a cantilever beam, when the tip mass M_T is added at the free end, the shear at the free end is given by $V - \omega^2 M_T w$. Equation (10) can also be written as

$$\begin{bmatrix} \nabla & 0 & 0 & \rho(x)A(x)\omega^2 \\ 0 & \nabla & \rho(x)I(x)\eta^2 & -P(x)\nabla \\ 0 & -\frac{1}{d(x)} & \nabla & 0 \\ -1 & 0 & -K(x) & (P(x)+K(x))\nabla \end{bmatrix} \times \begin{Bmatrix} V \\ M \\ \theta \\ w \end{Bmatrix} = \begin{Bmatrix} 0 \\ 0 \\ 0 \\ 0 \end{Bmatrix} \tag{11}$$

where

$$\eta^2 = \Omega^2 + \omega^2 \tag{12}$$

3 Differential transformation element method (DTEM)

In this section, the required mathematical background for better understanding of DTEM based dynamic stiffness method is presented.

If function $y(x)$ is analytic in domain D; let $x = x_0$ represent any point in the domain. Then Taylor's series expansion is given as

$$y(x) = \sum_{s=0}^{\infty} \frac{1}{s!} \left\{ \frac{\mathrm{d}^s y(x)}{\mathrm{d}x^s} \right\} \Bigg|_{x=x_0} (x - x_0)^s \tag{13a}$$

where s belongs to the set of non-negative integers denoted as S domain.

(a) Differential transformation DT of $y(x)$ is defined as $\bar{y}[s]$ as

$$\bar{y}[s] = \frac{1}{s!} \left\{ \frac{\mathrm{d}^s y(x)}{\mathrm{d}x^s} \right\} \Bigg|_{x=x_0} \tag{13b}$$

It is to be noted that differential transformation of any function is written in square brackets with a bar over the letter as shown in Eqs. (13a) and (13b).

(b) Inverse differential transformation (IDT): IDT is known as presentation of $y(x)$ by power series using DT of $y(x)$ as

$$y(x) = \sum_{s=0}^{\infty} \bar{y}[s](x - x_0)^s \tag{14a}$$

In practical problems, Eq. (14a) is replaced by a finite series as

$$y(x) = \sum_{s=0}^{nt} \bar{y}[s](x - x_0)^s \tag{14b}$$

where nt (number of terms) is chosen such that $y(x) = \sum_{s=nt+1}^{\infty} \bar{y}[s](x - x_0)^s$ is negligibly small. In this paper x_0 is set to zero.

If $y(x)$ is represented as polynomial expression as

$$y(x) = \sum_{s=0}^{nt} \mu_s (x - x_0)^s \tag{15a}$$

then one can identify $\bar{y}[0] = \mu_0$, $\bar{y}[1] = \mu_1 \ldots \bar{y}[nt] = \mu_{nt}$.

If $y(x)$ is a function $\bar{y}[0], \bar{y}[1], \ldots, \bar{y}[nt]$ can be determined using Eq. (13a).

The fundamental theorems of one dimensional differential transformation are

$$\begin{aligned} &w(x) = u(x) \pm v(x); && \bar{w}[s] = \bar{u}[s] \pm \bar{v}[s] \\ &w(x) = cu(x); && \bar{w}[s] = c\bar{u}[s] \quad \text{if } c \text{ is constant} \end{aligned}$$

If

$$\begin{aligned} &w(x) = u(x)v(x), \\ &\quad \bar{w}[s] = \sum_{i=0}^{s} \bar{u}[s-i]\bar{v}[i] \\ &w(x) = \frac{\mathrm{d}^p u(x)}{\mathrm{d}x^p}, \\ &\quad \bar{w}[s] = (s+1)(s+2)\ldots(s+p)\bar{u}[s+p] \end{aligned} \tag{15b}$$

Consider four first order differential equations over the domain $0 \le x \le L$. In order to solve the differential equation with Differential Transformation Element Method (DTEM), firstly a recurrent relation is obtained by using the IDT of each term in the differential equation and applying the theorems given above. It is possible to express $\bar{w}[s]$, $s = j, j+1, j+2, \ldots, nt$ in terms of $\bar{\theta}[s]$, $\bar{M}[s]$ and $\bar{V}[s]$, $s = 0, 1, 2, \ldots, j-1$ and centrifugal force term $\bar{P}[s]$, $s = 0, 1, 2, \ldots, j-1$ using the recurrent relation. Similarly $\bar{\theta}[s]$, $\bar{M}[s]$ and $\bar{V}[s]$ in terms of other three quantities and centrifugal force term $\bar{P}[s]$.

Assume Young's modulus E, mass density ρ, breadth of the cross section at any section 'b', depth of the section 'h' vary with respect to ξ as ($\xi = \frac{x}{L}$)

$$\begin{aligned} &E(\xi) = \left(a_1 + a_2\xi + a_3\xi^2\right); \\ &\rho(\xi) = \left(b_1 + b_2\xi + b_3\xi^2\right); \\ &b(\xi) = (c_1 + c_2\xi), \quad h(\xi) = (h_1 + h_2\xi) \end{aligned} \tag{16}$$

Hence area and moment of inertia vary as

$$\begin{aligned} &A(\xi) = area = b(\xi)h(\xi) = \left(e_1 + e_2\xi + e_3\xi^2\right); \\ &I = \left(f_1 + f_2\xi \ldots f_5\xi^4\right) \end{aligned} \tag{17}$$

Flexural rigidity $d(x) = E(x)I(x)$ and $\rho I(x) = \rho(x)I(x)$ are given by

$$d(\xi) = \left(g_1 + g_2\xi + g_3\xi^2 + g_4\xi^3 + \cdots + g_7\xi^6\right) \tag{18}$$

$$\rho I(\xi) = \left(q_1 + q_2\xi + q_3\xi^2 + q_4\xi^3 + \cdots + q_7\xi^6\right) \tag{19}$$

$\rho A(x)$ and $K(x)$ variation is given by

$$\begin{aligned} &\rho A(\xi) = \left(\alpha_1 + \alpha_2\xi \ldots \alpha_5\xi^4\right); \\ &K(\xi) = \left(\beta_1 + \beta_2\xi \ldots \beta_5\xi^4\right) \end{aligned} \tag{20}$$

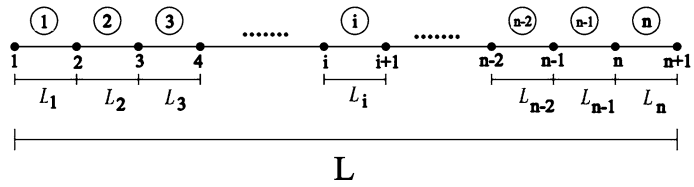

Fig. 2 DTEM model (numbers in circles and beneath the beam respectively denote element and node numbers)

Centrifugal force at any section is given by

$$P(\xi) = \Omega^2 RL \int_{\xi}^{1} \left(b_1 + b_2\xi + b_3\xi^2\right) \times \left(e_1 + e_2\xi + e_3\xi^2\right)(\delta + \xi)\,\mathrm{d}\xi = \left(\gamma_1 + \gamma_2\xi \ldots \gamma_7\xi^6\right) \tag{21}$$

From the above power series, we obtain

$$\begin{aligned} &\bar{d}[1] = g_1; \quad \bar{d}[2] = g_2 \ldots \bar{K}[1] = \beta_1; \\ &\bar{K}[2] = \beta_2; \quad \overline{\rho I}[1] = q_1; \quad \overline{\rho I}[2] = q_2 \\ &\overline{\rho A}[1] = \alpha_1; \quad \overline{\rho A}[2] = \alpha_2 \ldots \bar{P}[1] = \gamma_1; \\ &\bar{P}[2] = \gamma_2 \ldots \end{aligned} \tag{22}$$

In DTEM, the whole domain is firstly divided into 'ne' elements as shown in Fig. 2. The solution of the governing differential equation in each element, i.e. $w_i(x)$, $\theta_i(x)$, $M_i(x)$ and $V_i(x)$, $i = 1, 2, \ldots$ ne are sought. The stiffness matrix and the shape functions for lateral displacements and bending rotations are obtained automatically. Assume transverse displacement $w(x)$ and bending rotation $\theta(x)$ along the element length could be expressed in terms of nodal ones as

$$\begin{aligned} w(x) &= \sum_{j=1}^{4} \psi_j \Delta_j = \boldsymbol{\psi}^T \boldsymbol{\Delta} \\ \theta(x) &= \sum_{j=1}^{4} \phi_j \Delta_j = \boldsymbol{\Phi}^T \boldsymbol{\Delta} \end{aligned} \tag{23}$$

in which

$$\Delta = \{w_i \theta_i w_j \theta_j\} \tag{24}$$

$$\begin{aligned} \boldsymbol{\psi} &= \{\psi_1 \psi_2 \psi_3 \psi_4\}^T \\ \boldsymbol{\Phi} &= \{\phi_1 \phi_2 \phi_3 \phi_4\}^T \end{aligned} \tag{25}$$

where $\boldsymbol{\psi}$ are shown in Fig. 3.

With the help of kinetic energy, consistent mass could be derived as

$$M_{ij} = \int_0^{L_e} \left(\rho(x)A(x)\psi_i\psi_j + \rho(x)I(x)\phi_i\phi_j\right)\mathrm{d}x \tag{26}$$

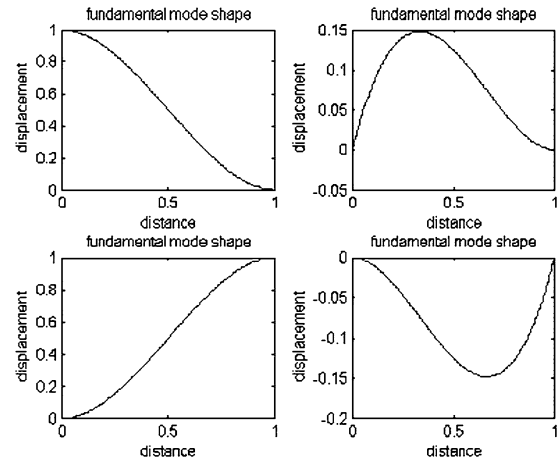

Fig. 3 Shape functions for nodal displacements

and geometric stiffness matrix is obtained as

$$KG_{ij} = \int_0^{L_e} \left(\frac{\mathrm{d}\psi}{\mathrm{d}x}\right)_i \left(\frac{\mathrm{d}\psi}{\mathrm{d}x}\right)_j \mathrm{d}x \tag{27}$$

Structural stiffness matrix is automatically obtained in DTEM.

3.1 Derivation of recurrent relation

To get DT of Eq. (11), the following two axioms are used. It is to be noted that from programming point of view $s = 1$ to nt is considered instead of $s = 0$ to nt in the usual way and nt denotes the number of terms. In all the numerical examples investigated, the number of terms considered is 40. The two axioms are

$$DT[AB] = \bar{A}[1] \times \bar{B}[s] + \sum_{i=2}^{s} \bar{A}[i] \times \bar{B}[s - i + 1] \tag{28}$$

and

$$\begin{aligned} DT\left[AB'\right] &= sA[1] \times B[s+1]/L \\ &\quad + \sum_{i=2}^{k} (s - i + 1) \times A[i] \times B[s - i + 2]/L \end{aligned} \tag{29}$$

where B' denotes $\frac{dB}{dx}$. From the last equation of Eq. (11)

$$-V - K(x)\theta + \big(P(x) + K(x)\big)\nabla w = 0 \tag{30}$$

Taking DT of the above equation and using the theorems we get

$$\bar{w}[s+1] = \frac{L}{s}\left\{\frac{(\bar{V}[s] + \bar{K}[1] \times \bar{\theta}[s] - s1)}{(\bar{P}[1] + \bar{K}[1])}\right\} \tag{31}$$

$s1$ in Eq. (31) is given by

$$\begin{aligned} s1 = -\sum_{i=2}^{s}\big\{&\bar{K}[i] \times \bar{\theta}[s-i+1] \\ &+ \big(\bar{P}[i] + \bar{K}[i]\big) \times (s-i+1) \\ &\times \bar{w}[s-i+2]/L\big\} \end{aligned} \tag{32}$$

From the third equation of Eqs. (11)

$$\begin{aligned} &-M + E(x)I(x)\nabla\theta = 0; \quad \text{or} \\ &-M + d(x)\nabla\theta = 0 \end{aligned} \tag{33}$$

Taking DT of the above equation we get

$$\bar{\theta}[s+1] = L\big\{\bar{M}[s] - s2\big\}/\big(s \times \bar{d}[1]\big) \tag{34}$$

where

$$s2 = \frac{1}{L}\sum_{i=2}^{k}(s-i+1)\bar{d}[i] \times \bar{\theta}[s-i+2] \tag{35}$$

From the second equation of Eqs. (11)

$$V + \nabla M + \rho(x)I(x)\eta^2\theta - P(x)\nabla w = 0 \tag{36}$$

Taking DT of the above equation we get

$$\begin{aligned} \bar{M}[s+1] = \frac{L}{s}\big\{&-\bar{V}[s] - \eta^2 \times \rho\bar{I}[1] \times \bar{\theta}[s] \\ &+ s \times \bar{P}[1] \times \bar{w}[s+1]/L - s3\big\} \end{aligned} \tag{37}$$

where

$$\begin{aligned} s3 = \eta^2 \sum_{i=2}^{k}\big\{&\overline{\rho I}[i] \times \bar{\theta}[s-i+1) \\ &- (s-i+1) \times \bar{P}[i] \times \bar{w}[s-i+2]/L\big\} \end{aligned} \tag{38}$$

From the first equation of Eqs. (11)

$$\nabla V + \omega^2\rho(x)A(x)w = 0 \tag{39}$$

Taking DT of the above equation, we get

$$\bar{V}[s+1] = -\omega^2 L\big\{\overline{\rho A}[1] \times \bar{w}[s] + s4\big\}/s \tag{40}$$

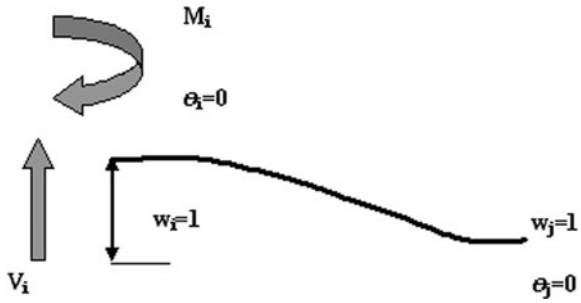

Fig. 4 Deformed shape unit lateral displacement at node i

where

$$\begin{aligned} &s4 = \omega^2 \sum_{i=2}^{s}\overline{\rho A}[i] \times \bar{w}[s-i+1] \\ &\rho A(x) = \rho(x)A(x) \end{aligned} \tag{41}$$

In the above equations $\bar{w}[1]$, $\bar{\theta}[1]$, $\bar{M}[1]$ and $\bar{V}[1]$ denote differential transformation values of deflection, bending rotation, moment and shear at the origin of the element. (In actual DTM, $\bar{w}[0]$, $\bar{\theta}[0]$, $\bar{M}[0]$ and $\bar{V}[0]$ are the deflection, rotation, moment and shear values at the origin of an element.) Using recurrence relation, obtain $\bar{w}[2], \bar{w}[3], \ldots, \bar{w}[nt], \ldots, \bar{V}[2], \bar{V}[3], \ldots, \bar{V}[nt]$ where 'nt' denotes the number of terms.

3.2 DTEM procedure to obtain shape functions, stiffness matrix, geometric stiffness matrix and mass matrices

Transverse displacements $w(x)$ and bending rotation $\theta(x)$ along element length could be expressed in terms of nodal ones as given by Eq. (23). Assume we want to get the shape function for $w_i = 1$ and all other displacements as zero. By recurrence relation for $\bar{w}[1] = 1$ and $\bar{M}[1] = 1$; $\bar{V}[1] = 1$ applied independently one can calculate the displacement $w_j = \sum_{s=1}^{nt}\bar{w}[s]$ at the right end of the element as p_1, y_1, and z_1 and calculate the rotation at the right end $\theta_j = \sum_{s=1}^{nt}\bar{\theta}[s]$ for the same $\bar{w}[1] = 1$ and $\bar{M}[1] = 1$; $\bar{V}[1] = 1$ applied independently as p_2, y_2, and z_2 respectively (see Fig. 4). To obtain the shape function for $w_i = 1$ along with the displacement we have transformation for moment M_i and shear V_i which can be obtained from compatibility equation as

$$\begin{bmatrix} y_1 & z_1 \\ y_2 & z_2 \end{bmatrix}\begin{Bmatrix} \bar{M}_i \\ \bar{V}_i \end{Bmatrix} + \begin{Bmatrix} p_1 \\ p_2 \end{Bmatrix} = \begin{Bmatrix} 0 \\ 0 \end{Bmatrix} \tag{42}$$

From Eq. (42) one can solve for $\bar{M}_i$, $\bar{V}_i$ and hence by knowing $\bar{w}_1$, $\bar{M}_1$, $\bar{V}_1$ one could obtain the shape function $\boldsymbol{\psi}$ by using recurrence relation. The same exercise is repeated for $\theta_i = 1$, $w_j = 1$ and $\theta_j = 1$. Similarly functions $\boldsymbol{\Phi}$ could also be obtained as shape functions for θ

$$\underset{4\times 1}{\boldsymbol{\psi}} = \underset{4\times nt}{\mathbf{uu}^T}\ \underset{nt\times 1}{\mathbf{xi}} \tag{43}$$

and

$$\underset{4\times 1}{\boldsymbol{\Phi}} = \underset{4\times nt}{\boldsymbol{\theta\theta}^T}\ \underset{nt\times 1}{\mathbf{xi}} \tag{44}$$

where

$$\mathbf{xi}^T = \left\langle 1\ \xi\ \xi^2\ \xi^3\ \xi^4\ \ldots\ \xi^{nt-1} \right\rangle \tag{45}$$

The mass matrix is obtained using Eq. (26) and in that

$$\rho A(\xi) = \overline{\rho A}[1] + \overline{\rho A}[2]\xi + \overline{\rho A}[3]\xi^2 \cdots \tag{46}$$

and

$$\rho I(\xi) = \overline{\rho I}[1] + \overline{\rho I}[2]\xi + \overline{\rho I}[3]\xi^2 \cdots. \tag{47}$$

The first term of the right hand side of Eq. (26) can be written as

$$M^I = \sum_{s=1}^{nt} L\left(\int_0^1 \left\{ \overline{\rho A}[s][uu]^T \mathbf{xixi}^T \xi^{s-1}[uu] \right\} d\xi \right)$$
$$= L \sum_{s=1}^{nt} \overline{\rho A}[s]\mathbf{uu}^T \mathbf{ax}^s \mathbf{uu} \tag{48}$$

The second term of mass matrix is obtained in a similar manner as

$$M^{II} = L \sum_{s=1}^{nt} \overline{\rho I}[s]\boldsymbol{\theta\theta}^T \mathbf{ax}^s \boldsymbol{\theta\theta} \tag{49}$$

Combining, the mass matrix is obtained as

$$M = L \sum_{s=1}^{nt} \overline{\rho A}[s]\mathbf{uu}^T \mathbf{ax}^s \mathbf{uu}$$
$$+ L \sum_{s=1}^{nt} \overline{\rho I}[s]\boldsymbol{\theta\theta}^T \mathbf{ax}^s \boldsymbol{\theta\theta} \tag{50}$$

wherein $\mathbf{ax}^s$

$$ax(i, j, s) = \frac{1}{(i + j + s - 2)} \tag{51}$$

$$\frac{d\psi}{dx} = \frac{1}{L}\mathbf{uu}^T \begin{Bmatrix} 0 \\ 1 \\ 2\xi \\ 3\xi^2 \\ \vdots \end{Bmatrix} = \frac{1}{L}\mathbf{uu}^T \mathbf{ay} \begin{Bmatrix} 1 \\ \xi \\ \xi^2 \\ \vdots \\ \vdots \end{Bmatrix} \tag{52}$$

where

$$\mathbf{ay} = \begin{bmatrix} 0 & 0 & \cdots & \cdots & 0 \\ 1 & 0 & \cdots & \cdots & 0 \\ 0 & 2 & \cdots & \cdots & 0 \\ 0 & 0 & 3 & \cdots & 0 \\ \vdots & \vdots & \vdots & \vdots & \vdots \end{bmatrix} \tag{53}$$

The geometric stiffness matrix is obtained using Eq. (27) as

$$\mathbf{KG} = \frac{1}{L}\mathbf{uu}^T \mathbf{ayax}^1 \mathbf{ay}^T \mathbf{uu} \tag{54}$$

Hence for an element, stiffness matrix [**K**], geometric stiffness [**KG**] and mass matrix [**M**] can be established. The element stiffness matrices are assembled to form global flexural stiffness matrix, global geometric stiffness matrix and global mass matrices. Boundary conditions are applied using Wilson's Lagrangian multiplier method [37] and the following equations are solved as eigen value problem for natural frequencies and buckling load.

$$[\mathbf{K}]\{r\} = \omega^2[\mathbf{M}]\{r\}; \qquad [\mathbf{K}]\{r\} = P_{cr}[\mathbf{KG}]\{r\} \tag{55}$$

4 Numerical results and discussion

The following problems can be investigated using the formulation developed in this paper.

(a) Free vibration of axially functionally graded tapered centrifugally stiffened Timoshenko beams
(b) Stability analysis of axially functionally graded tapered Timoshenko beams
(c) Free vibration analysis of axially functionally graded tapered Timoshenko beams
(d) By assuming very high shear stiffness (say 1e20) and neglecting rotary inertia, all the above three analyses can be carried out for Bernoulli–Euler beams.

4.1 Effects of variable cross section

Consider a tapered beam with a rectangular cross section whose breadth and height both taper vary linearly as

$$b = b_0(1 - c_b\xi); \qquad d = d_0(1 - c_h\xi) \tag{56}$$

where c_b and c_h are the taper parameters for the breadth and height.

Thus the cross sectional area and moment of inertia vary along the beam axis as (when $c_b = c_h = e$)

$$A = A_0(1 - e\xi)^{mr}; \qquad I = I_0(1 - e\xi)^{mr+2} \tag{57}$$

Case A. *Depth variation only* ($mr = 1$)

$$A = A_0(1 - e\xi); \qquad I = I_0(1 - e\xi)^3 \tag{58}$$

where $\xi = \frac{x}{L}$ is the non-dimensional longitudinal coordinate along the whole beam, L is the length of whole beam and e is taper ratio and A_0 and I_0 are respectively the values of cross-sectional area and moment of inertia at the root where $x = 0$.

Case B. *Both depth and breadth variation* ($mr = 2$)

$$A = A_0(1 - e\xi)^2; \qquad I = I_0(1 - e\xi)^4 \tag{59}$$

It is instructive to remember that the beam would be uniform when $e = 0$ and it would theoretically taper to a point if $e = 1$ and if e is negative, section depth and breadth increase from $x = 0$, i.e. ($\xi = 0$) to $x = L$, i.e. ($\xi = 1$).

4.2 Variation of material properties

Moreover, the distribution of modulus of elasticity and mass density are assumed to be respectively varied as power law distribution [38]. It is assumed that the axially FG beams is made of two constituents namely Aluminum and Zirconia with the following properties. (Poisson's ratio is assumed to be 0.3)

Al: $\mathrm{E} = 70$ GPa; $\rho = 2702\ \mathrm{kg/m^3}$

ZrO_2: $\mathrm{E} = 200$ GPa; $\rho = 5700\ \mathrm{kg/m^3}$

T is a typical material property such as E and ρ which is assumed to vary as

$$T = (T_a - T_z)\left(\frac{x}{L}\right)^{nr} + T_z \tag{60}$$

where the subscripts 'a' and 'z' refer to the values of the parameters for Aluminum and Zirconia respectively and nr is the material non-homogeneity parameter. The variation of E is depicted for a unit length of beam in Fig. 5 for different values of 'nr'. It is obvious that the percentage content of Zirconia increases as 'nr' increases towards infinity. It is recommended by Nakamura et al. [39] that nr varies in the range of $\frac{1}{3} \le nr \le 3$ and any value out of this range would result into a FG material with too high percentage of one of the constituents, here Zirconia.

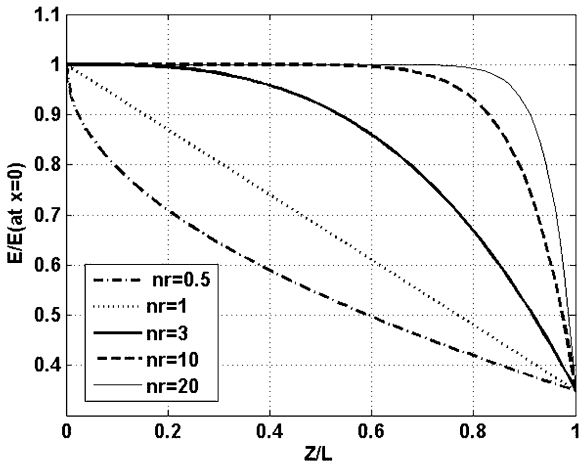

Fig. 5 Variation of Young's modulus along the beam axis with respect to different values of nr

In this section, several numerical examples are provided to demonstrate the competency of the present methods. In order to facilitate the presentation of results, the following dimensionless parameters are introduced as

Hub radius parameter: $\delta = \dfrac{R}{L}$

Rotary inertia parameter: $r^2 = \dfrac{I_0}{A_0 L^2}$

Rotating speed parameter: $\lambda = \Omega\sqrt{\dfrac{\rho_0 A_0 L^4}{E_0 I_0}}$

Tip mass parameter: $\beta = \dfrac{M_T}{\rho_0 A_0 L}$

Natural frequency parameter for graded beams:

$\mu = \omega\sqrt{\dfrac{\rho_0 A_0 L^4}{E_0 I_0}}$.

4.3 Convergence study

The competency of DT based dynamic stiffness (DS) method in free vibration of centrifugally stiffened tapered FG Timoshenko beams is verified through several numerical examples. In what follows, firstly the convergence of the DT based dynamic stiffness method (DT-DS) is examined. Afterwards, the effects of rotation speed, taper ratio, material non-homogeneity parameter on the natural frequencies are investigated.

It is very important to study the convergence characteristics of any numerical method to guarantee the

successful application of the method to various engineering problems. For the convergence study of (DT-DS) approach, an axially functionally graded centrifugally stiffened non-prismatic cantilever beam with the following parameters is considered. Since rectangle section is considered, shear correction factor may be assumed as 5/6.

$$\kappa = \frac{5}{6}; \qquad mr = 2; \qquad nr = 2;$$
$$G = 0.3846E; \qquad \delta = 0; \qquad \lambda = 5;$$
$$e = 0.8; \qquad r = \sqrt{\frac{I_0}{A_0}} = 0.08$$

Figure 6 shows the relation between the number of elements in (DT-DS) vs frequency parameter values. Considering four frequency parameters, $nt = 10$ terms would be sufficient to provide satisfactory results. However, for a highly nonlinear problem more number of terms may be necessary to achieve the required accuracy. Considering all the four frequency parameters 10 terms with 40 elements would be sufficient to solve the problem to a desired accuracy.

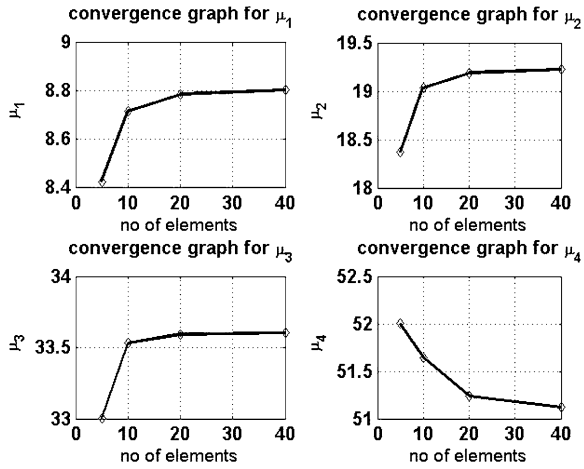

Fig. 6 Convergence characteristics of Dynamic stiffness method

4.4 Numerical examples

Example 1 (Uniform cantilever Timoshenko beam analysis ($r = \frac{1}{30}$)) The results of Table 1 illustrate the effect of the rotational speed parameter λ, on the fundamental natural frequency of the Timoshenko beam. The fundamental frequency values obtained by Dynamic stiffness method agree with Kaya [35] and Ozgumus and Kaya [40]. All the four fundamental frequencies increase with the increase in speed parameter. The values of ρ, E, A, L are assumed as unity and the shear correction factor κ is assumed as 5/6 and $G = 0.392E$. The hub radius is assumed to be equal to zero.

Example 2 Cantilever rotating Timoshenko beam with rotational speed parameter 4 ($mr = 1$; $\kappa = 2/3$ (circular section); $G = 0.375E$; $\delta = 0$; $\lambda = 4$) is considered. Table 2 illustrates the variation of natural frequencies of a rotating tapered Timoshenko beam with respect to the taper ratio and rotary inertia parameter 'r'. For $e = 0$, 0.25, 0.5, the frequency parameter values are

Table 1 Variation of the fundamental frequency parameters ($\mu = \sqrt{\frac{\rho AL^4\omega^2}{EI}}$) of a rotating Timoshenko cantilever beam for various value of λ (speed parameter) ($\lambda = \sqrt{\frac{\rho AL^4\Omega^2}{EI}}$ ($\delta = 0$, $r = \frac{1}{30}$, $\frac{E}{KG} = 3.059$))

λ	Method	μ_1	μ_2	μ_3	μ_4
0	Present	3.4798	20.5897	53.3587	95.3477
	Ref. [40]	3.4798	20.5891	53.3396	–
2	Present	4.0971	21.1772	53.9666	96.0345
	Ref. [40]	4.0971	21.1765	53.9542	–
4	Present	5.5314	22.8475	55.7700	98.0593
	Ref. [40]	5.5314	22.8466	55.7503	–
6	Present	7.2847	25.3817	58.6166	101.3223
	Ref. [50]	7.2848	25.3802	58.5978	101.2325
8	Present	9.1524	28.5402	62.3544	105.6805
	Ref. [50]	9.1524	28.5383	62.3331	105.5826
10	Present	11.0644	32.1276	66.8018	110.9715
	Ref. [50]	11.0643	32.1251	66.7797	110.8710

Table 2 Effect of rotary inertia and taper ratio parameters on the first six natural frequency parameters of tapered cantilever rotating Timoshenko beam ($\lambda = 4$; $\delta = 0$; $mr = 1$; $\kappa = 2/3$; $G = 0.375E$)

e	$\mu\backslash r$	0.01	0.02	0.04	0.06	0.08	0.10
0	μ_1	5.5791	5.5616	5.4951	5.3955	5.2750	5.1449
	μ_2	24.0993	23.6066	21.9574	19.9689	18.0661	16.3980
	μ_3	62.8313	59.8204	51.5031	43.7634	37.7601	33.2068
	μ_4	119.2481	109.5118	87.2835	70.2389	58.0473	47.8772
	μ_5	192.0369	169.5774	126.5043	97.8983	77.6885	58.9470
	μ_6	279.5836	236.3005	167.4769	124.5188	86.4281	66.3281
0.25	μ_1	5.6955	5.6793	5.6176	5.5238	5.4089	5.2832
	μ_2	22.4245	22.0606	20.8062	19.2211	17.6409	16.2201
	μ_3	56.2869	54.1231	47.7641	41.3932	36.2109	32.2086
	μ_4	105.9175	98.8808	81.4300	67.0090	56.5291	48.5809
	μ_5	170.3942	153.9025	119.1292	94.4127	77.6753	63.8540
	μ_6	248.5546	216.9176	159.0911	122.3688	94.3178	67.1142
0.5	μ_1	5.8737	5.8585	5.8002	5.7106	5.5989	5.4746
	μ_2	20.5979	20.3447	19.4441	18.2468	16.9922	15.8208
	μ_3	49.1315	47.6995	43.2071	38.3024	34.0490	30.6380
	μ_4	91.1103	86.4626	73.8248	62.3342	53.5745	47.0082
	μ_5	145.9774	134.9248	108.9238	88.6167	74.3941	64.1896
	μ_6	212.9662	191.3196	146.8746	116.0289	95.3126	73.3436

read approximately from Fig. 4 of Ozgumus and Kaya [40] and compared with the present results in Table 2 and the agreement is quite good. When the rotary inertia parameter increases, the natural frequency parameter μ decreases. Although decreases, the product of μr still increase and hence natural frequency increases. Rotary inertia parameter has dominant effect on higher modes. It is also seen that lower mode frequency parameters are not affected with increase in 'r' whereas there is remarkably high decrease in higher mode frequency parameter values. The taper ratio has decreasing effect on natural frequency parameters.

Example 3 Consider a tapered axially FG Timoshenko beam with $\delta = 0$ rotating with a speed of $\lambda = 5$. The material follows power law with $nr = 2$. The first four dimensionless natural frequency parameters of the beam are tabulated in Table 3 for $mr = 2$. It can be verified that the frequency parameter values for all types of boundary conditions investigated decrease with taper ratio except for C-F condition where it shows an increasing trend. The first four normalized mode shapes of the beam with taper ratios $e = 0$, 0.8 are given in Fig. 7 for $mr = 1$, $nr = 2$ for C-F boundary conditions and these four normalized mode shapes compare well qualitatively with Fig. 7 of Ref. [41].

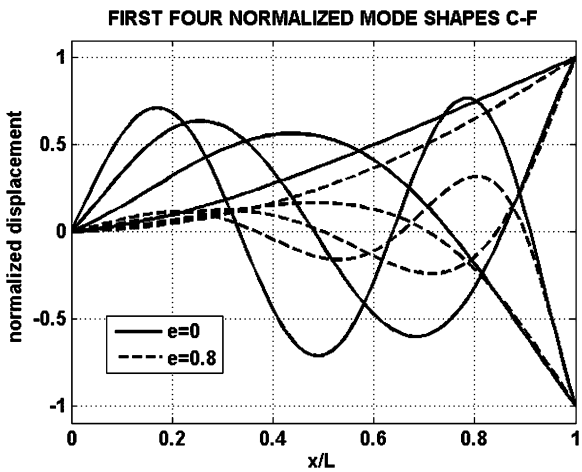

Fig. 7 The first four normalized mode shapes (*solid line*: $e = 0$; *dotted line*: $e = 0.8$) of an axially graded rotating tapered Timoshenko beam with $\lambda = 2$; $\delta = 0$; and $mr = nr = 2$: Boundary Condition C-F

Example 4 Table 4 shows the buckling loads of a non rotating homogeneous uniform Timoshenko column ($r = 0.1$; $\kappa = 5/6$; $G = 0.3846E$) and the results agree with Wang et al. [42].

Example 5 Time history analysis of a simply supported Timoshenko beam subjected to step loading at mid span of the beam ($L = 10$ m; $b = 0.1$ m; $h =$

Table 3 Effect of taper ratio on fundamental frequency parameters of rotating axially FG Timoshenko beam with different BCS ($r = 0.08$; $mr = 2$; $nr = 2$; $\kappa = 5/6$; $G = 0.3846E$; $\lambda = 5$)

BCS	μ	Method\e	0	0.2	0.4	0.6	0.8
C-F	μ_1	Present	6.5492	6.8456	7.2476	7.8363	8.8046
		Ref. [50]	6.5490	6.8455	7.2477	7.8375	8.8103
	μ_2	Present	20.1634	19.9545	19.6601	19.3307	19.2247
		Ref. [50]	20.1594	19.9507	19.6569	19.3170	19.2635
	μ_3	Present	40.4996	39.2292	37.6905	35.8192	33.6024
		Ref. [50]	40.4696	39.2011	37.6655	35.8002	33.6037
	μ_4	Present	62.2050	60.6617	58.4054	55.3384	51.1202
		Ref. [50]	62.1017	60.5612	58.3131	55.2606	51.0782
C-P	μ_1	Present	14.0328	13.5267	12.9208	12.1967	11.3448
		Ref. [50]	14.0314	13.5256	12.9202	12.1971	11.3482
	μ_2	Present	33.4846	32.0707	30.3854	28.3053	25.5703
		Ref. [50]	33.4670	32.0551	30.3725	28.2966	25.5713
	μ_3	Present	55.6102	53.5175	50.9386	47.6127	42.9311
		Ref. [50]	55.5302	53.4452	50.8759	47.5631	42.9053
	μ_4	Present	78.3744	76.1937	73.0856	68.8491	62.5113
		Ref. [50]	78.1607	75.9876	72.9007	68.6944	62.4072
C-C	μ_1	Present	16.2510	15.4826	14.5651	13.4538	12.0895
		Ref. [50]	16.2489	15.4809	14.5640	13.4538	12.0919
	μ_2	Present	34.8109	33.6254	32.0858	29.9958	26.9365
		Ref. [50]	34.7911	33.6073	32.0703	29.9844	26.9337
	μ_3	Present	56.2017	54.4807	52.29581	49.3064	44.6603
		Ref. [50]	56.1192	54.4041	52.2298	49.2500	44.6258
	μ_4	Present	78.3768	76.5054	73.9286	70.2859	64.3744
		Ref. [50]	78.1624	76.2979	73.7369	70.1197	64.2439
P-P	μ_1	Present	11.1496	10.2250	9.1372	7.8499	6.3271
		Ref. [50]	11.1490	10.2245	9.1372	7.8505	6.3295
	μ_2	Present	30.9399	29.0945	26.9534	24.4290	21.3636
		Ref. [50]	30.9261	29.0829	26.9447	24.4244	21.3674
	μ_3	Present	53.9994	51.5652	48.5295	44.7684	39.6664
		Ref. [50]	53.9261	51.5000	48.5352	44.7738	39.6496
	μ_4	Present	77.9281	75.3004	71.8307	67.1910	60.3614
		Ref. [50]	77.7108	75.0993	71.6545	67.0478	60.2707

Table 4 Buckling load parameters of homogeneous Timoshenko column for various boundary conditions ($r = 0.1$, $G = 0.3846E$, $\kappa = 5/6$)

Method	Cantilever	Simply supported	Clamped-pinned	Clamped-clamped
Present	2.2910	7.5466	11.9421	17.6982
Ref. [42]	2.2912	7.5459	11.9421	17.6892

0.1 m; $E = 2.058 \times 10^{11}\,\mathrm{N\,m^{-2}}$, $\nu = 0.3$; $\kappa = 5/6$; $\rho = 7860\,\mathrm{kg\,m^{-3}}$; $F(t) = 300\,\mathrm{N}$ at mid span of the beam). Figure 8 shows the vertical response at the mid span of the beam for the first 5.0 seconds and compares well qualitatively with the results obtained by Tang [43]. Tang [43] used Leung's equation to derive the overall mass and stiffness matrix which is more suitable for response analysis than the overall dynamic stiffness matrix. Tang [43] obtained the results of forced vibration of the beam by the precise time

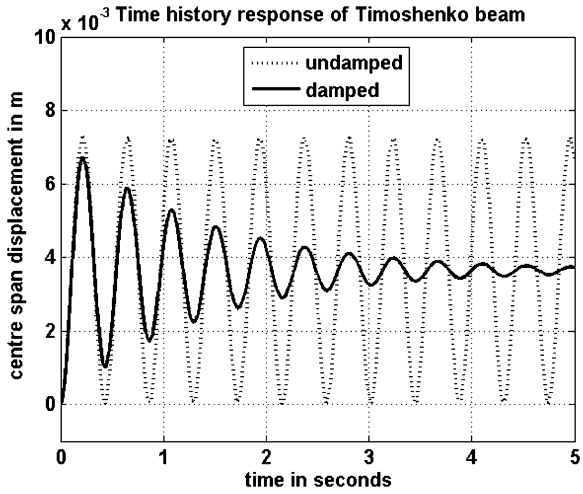

Fig. 8 Forced vibration response of a simply supported Timoshenko beam

integration method of Zhong and Williams [44]. But in the present analysis, considering only first five fundamental modes, the mass and stiffness matrices are reduced to the size of 5×5 and forced vibration analysis is carried out by using Newmark's linear acceleration method with step size of 0.005 seconds up to 5 seconds. For comparison, forced response for damped system (with damping factor $\varsigma = 0.05$) is also carried out for the same beam and plotted in Fig. 8.

Example 6 Consider an axially FG tapered non rotating Timoshenko beam with material non-homogeneity parameter $nr = 2$. The first four frequency parameters of the beam with C-F, H-H; and C-C boundary conditions are given in Table 5. The results agree well with those of Shahba et al. [27].

Table 5 The first four dimensionless frequency parameters and buckling load parameter of an axially FG tapered Timoshenko beam with different BCS ($nr = 2$; $mr = 2$; $r = 0.1$)

BCS	e	Method	μ_1	μ_2	μ_3	μ_4	p
CF	0	Present	3.8830	15.2620	31.6426	47.7114	1.9813
		Ref. [27]	3.8828	15.2589	31.6177	47.6343	–
	0.2	Present	4.2382	15.3421	31.0386	47.6000	1.4449
		Ref. [27]	4.2384	15.3441	31.0546	47.6550	1.4455
	0.4	Present	4.7112	15.3532	30.2315	46.6905	0.9334
		Ref. [27]	4.7121	15.3573	30.2496	46.7483	0.9344
	0.6	Present	5.3900	15.3363	29.1692	45.0504	0.4745
		Ref. [27]	5.3931	15.3467	29.1962	45.1172	0.4759
	0.8	Present	6.4908	15.5230	27.8439	42.4777	0.1301
		Ref. [27]	6.5009	15.5568	27.9102	42.5941	0.1317
H-H	0	Present	7.9877	24.2638	42.3642	54.9263	5.5372
		Ref. [27]	7.9872	24.2521	42.3024	54.8771	–
	0.2	Present	7.2225	23.1257	41.0674	57.3713	3.4698
		Ref. [27]	7.2245	23.1398	41.1243	59.5225	3.4735
	0.4	Present	6.2718	21.7254	39.3424	57.6395	1.8664
		Ref. [27]	6.2755	21.7423	39.3994	57.7881	1.8702
	0.6	Present	5.0640	19.9664	36.9684	54.9521	0.7671
		Ref. [27]	5.0709	19.9917	37.0337	55.1026	0.7707
	0.8	Present	3.4305	17.6686	33.4251	50.5663	0.1670
		Ref. [27]	3.4452	17.7204	33.5322	50.7616	0.1697
C-C	0	Present	12.6890	26.6569	43.4356	59.4149	11.3147
		Ref. [27]	12.6873	26.6413	43.3688	59.2779	–
	0.2	Present	12.2382	26.1318	42.5980	59.3868	7.2973
		Ref. [27]	12.2429	26.1524	42.6634	59.5335	7.3377
	0.4	Present	11.6616	25.3678	41.4674	58.3744	4.1313
		Ref. [27]	11.6683	25.3905	41.5341	58.5279	4.1590
	0.6	Present	10.9084	24.1968	39.7889	56.5047	1.8451
		Ref. [27]	10.9200	24.2270	39.8636	56.6668	1.8590
	0.8	Present	9.8941	22.2401	36.8881	52.9827	0.4589
		Ref. [27]	9.9207	22.3010	37.0050	53.1931	0.4650

Table 6 Predictions of non-dimensional natural frequency $\mu^2 = \frac{\rho A_0 \omega^2 L^4}{EI_0}$ of a tapered cantilever beam under different rotation speeds $\rho A(x) = \rho A_0(1 - 0.5x/L)$; $EI(x) = EI_0(1 - 0.5x/L)$ where $\lambda^2 = \frac{\rho A_0 \Omega^2 L^4}{EI_0}$

λ	I mode		II mode		III mode	
	Present	Ref. [7]	Present	Ref. [7]	Present	Ref. [7]
0	3.8238	3.8238	18.3173	18.3173	47.2649	47.2648
2	4.4368	4.4368	18.9366	18.9366	47.8717	47.8716
4	5.8788	5.8788	20.6852	20.6852	49.6457	49.6456
6	7.6551	7.6551	23.3093	23.3093	52.4633	52.4633
8	9.5540	9.5540	26.5437	26.5437	56.1596	56.1595
10	11.5015	11.5015	30.1828	30.1827	60.5640	60.5639

Example 7 In this example, we consider a tapered rotating Euler beam with cantilevered boundary conditions. Wright et al. [11] and Hodges and Rutkowski [45] studied the same example. Wang and Wereley [7] used only one single SFEM with 80 terms in the Frobenius power series to obtain the natural frequencies. The mass distribution was assumed to be linear as $\rho(x) = \rho_0(1-0.5\xi)$ and the flexural stiffness $EI(x)$ as $EI(x) = EI_0(1-0.5\xi)^3$. This is a depth tapered beam with depth taper ratio as 0.5. All the three modal frequencies as shown in Table 6 exactly match with Wang and Wereley [7] where the rotation speed varies from 0 to 10. Banerjee [8] also studied the same example using uniform rotating dynamic stiffness method where 20 elements were included. In this paper, for a tapered beam exact displacement function is obtained in DT based Dynamic stiffness method.

Example 8 (Axially FG beam with $\delta = 0$ and $\lambda = 2$) The material follows the power law with $nr = 2$. The first four non-dimensional natural frequencies of the beam are tabulated in Table 7 for $mr = 1$ (depth tapered beam) and compared with Zarrinzadeh et al. [46] who solved the problem by Finite element approach and the agreement is very good. It is generally observed that the natural frequencies for all types of boundary conditions decrease with taper ratio with some exceptions. The fundamental frequency increases with respect to taper ratio for C-F condition. These effects are also observed for homogeneous rotating beams by Attarnejad and Shahba [29].

Example 9 Table 8 shows the results of free vibration analysis of axially functionally graded Euler beam ($E = E_0(1+\xi)$, $\rho = \rho_0(1+\xi+\xi^2)$) ($mr = 2$) by (DT-DS) method and compared with Shahba et al. [27]. It is observed that all natural frequencies decrease with the increase in taper ratio except for the fundamental mode of C-F boundary condition. This exception has been also well pointed out by Ozgumus and Kaya [47] for homogeneous tapered beams in the literature.

Example 10 (Buckling load of axially functionally graded column) As a comparison, we consider the flexural rigidity of the column is of the form $EI(x) = EI_0(1 + \xi - \xi^2)$ where EI_0 is the flexural rigidity of the column at $\xi = 0$. Elishakoff [48] has given the exact buckling load as $P_{cr} = \frac{12EI_0}{L^2}$. But no closed form solution is available for the same column with other boundary conditions. Huang and Li [49] used Fredholm integral equation and obtained the buckling loads for columns with various boundary conditions and the results of the present analysis are compared with Huang and Li [49] in Table 9 and the agreement is quite good.

Example 11 (Buckling load of axially functionally graded column) We consider two special flexural rigidities of polynomial form, one being linearly varying flexural rigidity $EI(x) = EI_0(1 + \xi)$ and the other being parabolically varying flexural rigidity $EI(x) = EI_0(1 + \xi)^2$. The results obtained by the present analysis are compared in Table 9 with Huang and Li [49] and they are in excellent agreement with the published results.

Table 7 Effect of taper ratios on the natural frequency parameters of rotating axially functionally graded Euler beam ($mr = 1$, $nr = 2$, $\lambda = 2$)

BCS	μ	Method\e	0.0	0.2	0.4	0.6	0.8
C-C	μ_1	Present	20.8998	18.9040	16.7755	14.4417	11.7191
		Ref. [46]	20.8998	18.9039	16.7754	14.4416	11.7191
	μ_2	Present	58.5678	52.7377	46.5184	39.6926	31.7054
		Ref. [46]	58.5674	52.7373	46.5180	39.6923	31.7051
	μ_3	Present	115.6549	103.9306	91.4119	77.6530	61.5112
		Ref. [46]	115.6540	103.9298	91.4111	77.6523	61.5106
	μ_4	Present	191.8589	172.2437	151.2891	128.2418	101.1657
		Ref. [46]	191.8573	173.2422	151.2878	128.2405	101.1646
P-P	μ_1	Present	10.0557	9.0058	7.8656	6.5869	5.0513
		Ref. [46]	10.0556	9.0057	7.8655	6.5869	5.0513
	μ_2	Present	38.8041	34.9068	30.8038	26.3822	21.3557
		Ref. [46]	38.8038	34.9066	30.8036	26.3819	21.3555
	μ_3	Present	86.5675	77.7549	68.4207	58.2758	46.5910
		Ref. [46]	86.5667	77.7542	68.4201	57.2753	46.5905
	μ_4	Present	153.3802	137.6545	120.9408	102.6888	81.5051
		Ref. [46]	153.3789	137.6533	120.9397	102.6878	81.5042
C-F	μ_1	Present	4.8142	4.9117	5.0459	5.2477	5.6035
		Ref. [46]	4.8142	4.9116	5.0458	5.2470	5.6034
	μ_2	Present	23.6964	22.1973	20.6027	18.8878	17.0531
		Ref. [46]	23.6964	22.1971	20.6025	18.8876	17.0528
	μ_3	Present	62.2947	56.7757	50.9236	44.5820	27.4282
		Ref. [46]	62.2940	56.7751	50.9230	44.5815	37.4277
	μ_4	Present	119.7210	108.2365	96.0219	82.7028	67.4070
		Ref. [46]	119.7198	108.2354	96.0209	82.7019	67.4062
C-P	μ_1	Present	15.6599	14.4883	13.2189	11.8004	10.1039
		Ref. [46]	15.6598	14.4881	13.2188	11.8003	10.1038
	μ_2	Present	49.0113	44.4589	39.6089	34.2992	28.1229
		Ref.[46]	49.0109	44.4585	39.6085	34.2929	28.1226
	μ_3	Present	101.5241	91.5529	80.9228	69.2731	55.6961
		Ref. [46]	101.5232	91.5521	80.9221	69.2725	55.6955
	μ_4	Present	173.0918	155.7085	137.1607	116.8062	93.0203
		Ref. [46]	173.0903	155.7070	137.1594	116.8050	93.0193

5 Conclusions

For uniform Cantilever Timoshenko rotating beam analysis the fundamental frequency parameter values obtained by Dynamic Stiffness method agree with Kaya [35] and Ozgumus and Kaya [40]. All the four fundamental frequencies increase with the increase in speed parameter.

It is also seen that lower mode frequencies are not affected with increase in 'r' whereas there is remarkably high decrease in higher mode frequency values. The taper ratio has decreasing effect on natural frequencies.

It can be verified that the frequency values for all types of boundary conditions investigated decrease with taper ratio except for C-F condition where it shows an increasing trend.

For non rotating homogeneous uniform Timoshenko column ($r = 0.1$; $\kappa = 5/6$; $G = 0.3846E$) the buckling loads calculated agree with Wang et al. [42].

Table 8 Non-dimensional transverse frequencies ($\mu = \sqrt{\frac{\rho A_0 L^4 \omega^2}{EI_0}}$) for an axially FG tapered beam; Boundary Condition: C-C; Mode: 1–2 ($EA = EA_0(1+\xi)$; $\rho A = \rho A_0(1+\xi+\xi^2)$, $mr = 2$ (μ—frequency parameter); p = buckling load parameter = $\frac{P_{cr} L^2}{EI_0}$)

BCS	μ/p	Method\e	0	0.2	0.4	0.6	0.8
C-F	μ_1	Present	2.4256	2.6863	3.0484	3.5976	4.5651
		Ref. [51]	2.4256	2.6863	3.0486	3.5985	4.5695
	μ_2	Present	18.6041	17.7500	16.8562	15.9586	15.2814
		Ref. [51]	18.6042	17.7501	16.8571	15.9616	15.2955
	p	Present	3.1177	2.4638	1.7988	1.1208	0.4440
		Ref. [51]	3.1177	2.4638	1.7988	1.1208	0.4441
C-C	μ_1	Present	20.4721	18.1994	15.8343	13.3216	10.5256
		Ref. [51]	20.4721	18.1996	15.8350	13.3238	10.5339
	μ_2	Present	56.5482	50.4552	44.0341	37.1026	29.2089
		Ref. [51]	56.5491	50.4565	44.0370	37.1104	29.2402
	p	Present	57.3940	37.6024	21.7813	10.0640	2.6650
		Ref. [51]	57.3948	37.6028	21.7817	10.0645	2.6649
P-P	μ_1	Present	9.0286	8.1461	7.1251	5.8860	4.2265
		Ref. [51]	9.0286	8.1462	7.1254	5.8867	4.2283
	μ_2	Present	36.3715	32.5118	28.4989	24.2429	19.5172
		Ref. [51]	36.3717	32.5123	28.5003	24.2469	19.5300
	p	Present	14.5113	9.5971	5.6228	2.6338	0.7075
		Ref. [51]	14.5113	9.5171	5.6228	2.6338	0.7078

Table 9 Critical buckling load parameter of a FG Euler column for various BCS

BCS	$EI = EI_0(1+\xi-\xi^2)$		$EI = EI_0(1+\xi)$		$EI = EI_0(1+\xi)^2$	
	Present	Ref. [49]	Present	Ref. [49]	Present	Ref. [49]
C-F	2.863751	2.863571	3.117696	3.117696	3.836377	3.836377
P-P	12.000000	12.000000	14.511250	14.511250	20.792290	20.792288
C-P	23.664382	23.664377	29.448970	29.448963	42.109190	42.109176
C-C	45.395645	45.395607	57.394010	57.393956	81.923469	81.923363

For axially functionally graded Euler beam ($E = E_0(1+\xi)$, $\rho = \rho_0(1+\xi+\xi^2)$) ($mr = 2$) it is observed that all natural frequencies decrease with the increase in taper ratio except for the fundamental mode of C-F boundary condition.

Regarding the DT-DS method the following conclusions are arrived at.

DTM exactly coincides with the traditional Taylor series method when it is applied to problems involving ordinary differential equations [52]. This method captures the effects of variable cross section, centrifugal force and the material non-homogeneity parameter due to axially graded material. Since Wilson's Lagrangian multiplier method is used, it is easy to incorporate the boundary conditions. DT-DS method considers four first order differential equations instead of one fourth order differential equation and hence writing the Differential transform is an easy task. This method is superior to many other methods because of its simplicity and accuracy in calculating natural frequencies and buckling load and plotting the mode shapes also.

It was shown in the paper that an efficient finite element could be developed based on structural mechanics principles. Instead of assuming shape functions before hand as in classical finite element method, in the

DT-DS method proposed, shape functions are derived using DTM satisfying overall equilibrium and compatibility of a beam. Hence they represent real deformations which depend on the variation of material properties such as modulus of elasticity and mass density, variation of geometry (b, h) of the beam. These deformations (shape functions) are substituted in the potential and kinetic energy expressions to derive the stiffness and mass matrices to carry out static and free and forced vibration analysis. Since the new shape functions were derived based on the static deformations, in static problem exact results were obtained by using two elements whereas in dynamic problem at least 10 elements are needed to get the accurate result. Though there are many methods proposed to find the shape functions, a DTM based method is simple, precise and easy to use compared to many other methods developed. Since DT based Dynamic Stiffness method (DT-DS) is efficient tool for solving nonlinear or parameter varying systems, it is expected that this method will find a wide range of applications in structures of functionally graded materials.

Acknowledgements The author thanks the management and Principal Dr. R. Rudramoorthy of PSG College of Technology for providing necessary facilities to complete the research work reported in this paper. The author also thanks the anonymous reviewers for their advice and suggestions towards enhancing the quality of the manuscript.

References

1. Koizumi M (1993) The concept of FGM. Ceramic Trans Funct Grad Mater 34:3–10
2. Koizumi M (1997) FGM activities in Japan. Composites, Part B, Eng 28:1–4
3. Elishakoff I, Perez A (2005) Design of a polynomially inhomogeneous bar with a tip mass for specified mode shape and natural frequency. J Sound Vib 287(4–5):1004–1012
4. Elishakoff I, Pentaras D (2006) Apparently the first closed-form solution of inhomogeneous elastically restrained vibrating beams. J Sound Vib 298(1–2):439–445
5. Banerjee JR (1997) Dynamic stiffness formulation for structural elements: a general approach. Comput Struct 63:101–103
6. Banerjee JR (2000) Free vibration of centrifugally stiffened uniform and tapered beams using the dynamic stiffness method. J Sound Vib 233(5):857–875
7. Wang G, Wereley NM (2004) Free vibration analysis of rotating blades with uniform tapers. AIAA J 42(12):429–437
8. Banerjee JR, Su H, Jackson DR (2006) Free vibration of rotating tapered beams using the dynamic stiffness method. J Sound Vib 298(4–5):1034–1054
9. Vinod KG, Gopalakrishnan S, Ganguli R (2007) Free vibration and wave propagation analysis of uniform and tapered rotating beams using spectrally formulated finite elements. Int J Solids Struct 44:5875–5893
10. Doyle JF (1977) Wave propagation in structures, 2nd edn. Springer, Berlin (Chap 5)
11. Wright AD, Smith VR, Thresher TW, Wang JLC (1982) Vibration modes of centrifugally stiffened beams. ASME J Appl Mech 49(2):197–202
12. Huang Y, Li XF (2010) A new approach for free vibration of axially functionally graded beams with non-uniform cross section. J Sound Vib 329(11):2291–2303
13. Mabie HH, Rogers CB (1972) Transverse vibration of double-tapered cantilever beams. J Acoust Soc Am 51:1771–1774
14. Downs B (1977) Transverse vibration of cantilever beam having unequal breadth and depth tapers. ASME J Appl Mech 44:737–742
15. Gupta RS, Rao SS (1978) Finite element eigen value analysis of tapered and twisted Timoshenko beams. J Sound Vib 56(2):187–200
16. Dawe DJ (1978) A finite element for the vibration analysis of Timoshenko beams. J Sound Vib 60(1):11–20
17. To CWS (1981) A linearly tapered beam finite element incorporating shear deformation and rotary inertia for vibration analysis. J Sound Vib 78(4):475–484
18. Lees AW, Thomas DL (1982) Unified Timoshenko beam finite element. J Sound Vib 80(3):355–366
19. Lee SY, Lin SM (1994) Bending vibrations of rotating nonuniform Timoshenko beams with an elastically restrained root. ASME J Appl Mech 61:949–955
20. Du H, Lim MK, Liew KK (1994) A power series solution for vibration of a rotating Timoshenko beam. J Sound Vib 175(4):505–523
21. Nagaraj VT (1996) Approximate formula for the frequencies of a rotating Timoshenko beam. J Aircr 33:637–639
22. Lin SC, Hsiao KM (2001) Vibration analysis of a rotating Timoshenko beam. J Sound Vib 240(2):303–322
23. Choi DT, Chou YT (2001) Vibration analysis of elastically supported turbo machinery blades by the modified differential quadrature methods. J Sound Vib 240(5):937–953
24. Irie T, Yamada G, Takahashi I (1979) Determination of the steady state response of a Timoshenko beam of varying section by the use of the spline interpolation technique. J Sound Vib 63(2):287–295
25. Irie T, Yamada G, Takahashi I (1980) Vibration and stability of a non-uniform Timoshenko beam subjected to follower force. J Sound Vib 70(4):503–512
26. Lee SY, Lin SM (1992) Exact vibration solutions for nonuniform Timoshenko beams with attachments. AIAA J 30(12):2930–2934
27. Shahba A, Attarnejad R, Tavanaie Marvi M, Hajilar S (2011) Free vibration and stability of axially functionally graded tapered Timoshenko beams with classical and nonclassical boundary conditions. Composites, Part B, Eng 42(4):801–808
28. Attarnejad R, Semnani SJ, Shahba A (2010) Basic displacement functions for free vibration analysis of non-prismatic Timoshenko beams. Finite Elem Anal Des 46:916–929
29. Attarnejad R, Shahba A (2011) Basic displacement functions for centrifugally stiffened tapered beam. Int J Numer Methods Biomed Eng 27:1385–1397

30. Attarnejad R, Shahba A (2011) Basic displacement functions in analysis of centrifugally stiffened tapered beams. Arab J Sci Eng 36:841–853
31. Zhou JK (1986) Differential transformation and its application for electrical circuits. Huazhong University Press, China
32. Chen CK, Ju SP (2004) Application of differential transformation to transient advective-dispersive transport equation. J Appl Math Comput 155(1):25–38
33. Arikoglu A, Ozkol I (2004) Solution of boundary value problems for integro-differential equations by using differential transformation method. J Appl Math Comput 168(2):1145–1158
34. Bert CW, Zeng H (2004) Analysis of axial vibration of compound bars by differential transformation method. J Sound Vib 275(3–5):641–647
35. Kaya MO (2006) Free vibration analysis of a rotating Timoshenko beam by differential transformation method. Aircr Eng Aerosp Technol 78:194–203
36. Banerjee JR, Sobey AJ (2002) Energy expressions for rotating tapered Timoshenko beam. J Sound Vib 254(4):818–822
37. Wilson EL (2002) Three dimensional static and dynamic analysis of structures. Computers and Structures, Berkeley
38. Wakashima K, Hirano T, Nino M (1990) Space applications of advanced structural materials. ESA SP 303:97
39. Nakamura T, Wang T, Sampath S (2000) Determination of properties of graded materials by inverse analysis and instrumented indentation. Acta Mater 48:4293–4306
40. Ozgumus OO, Kaya MO (2010) Vibration analysis of a rotating tapered Timoshenko beam using DTM. Meccanica 45:33–42
41. Attarnejad R, Shahba A (2011) Dynamic displacement functions in free vibration analysis of centrifugally stiffened tapered beams. Meccanica 46(6):1267–1281
42. Tang B (2008) Combined dynamic stiffness matrix and precise time integration method for transient forced vibration response analysis of beams—short communication. J Sound Vib 309:868–876
43. Zhong WX, Williams FW (1994) A precise time step integration method. Proc IME C J Mech Eng Sci 208:427–430
44. Wang CM, Wang CY, Reddy JN (2005) Exact solutions for buckling of structural members. CRC Press, Boca Raton
45. Hodges DH, Rutkowski MJ (1981) From vibration analysis of rotating beam by a variable order finite element method. AIAA J 19:1459–1466
46. Zarrinzadeh H, Attarnejad R, Shahba A (2012) Free vibration of rotating axially functionally graded tapered beams. Proc IME G J Aero Eng 226(4):363–379
47. Ozgumus OO, Kaya MO (2006) Flapwise bending vibration analysis of double tapered rotating Euler-Bernoulli beam by using the differential transform method. Meccanica 41:661–670
48. Elishakoff I (2001) Inverse buckling problem for inhomogeneous columns. Int J Solids Struct 38(3):457–464
49. Huang Y, Li XF (2011) Buckling analysis of nonuniform and axially graded columns with varying flexural rigidity. ASCE J Eng Mech 137(1):73–81
50. Rajasekaran S (2012) Free vibration of centrifugally stiffened axially functionally graded tapered Timoshenko beams using differential transformation and quadrature methods. Appl Math Model. doi:10.1016/j.apm.2012.09.024
51. Shahba A, Rajasekaran S (2012) Free vibration and stability of tapered Euler-Bernoulli beams made of axially functionally graded materials. Appl Math Model 36:3094–3111
52. Bervillier (2012) State of the differential transformation method. J Appl Math Comput 218:10158–10170